

Supporting Information

Heterocyclic amine directed synthesis of metal(II)-oxalates: investigating the magnetic properties of two complete series of chains with $S = \frac{5}{2}$ to $S = \frac{1}{2}$

Tony D. Keene,^{a-d*} Iwan Zimmermann,^b Antonia Neels,^e Olha Sereda,^e Jürg Hauser,^b Michel Bonin,^b Michael B. Hursthouse,^c Daniel J. Price^{d*} and Silvio Decurtins.^{b*}

Figure S1 $\pi\cdots\text{H}$ interaction in **4** with average $\text{H}\cdots\text{C}$ distance of 3.11 Å.

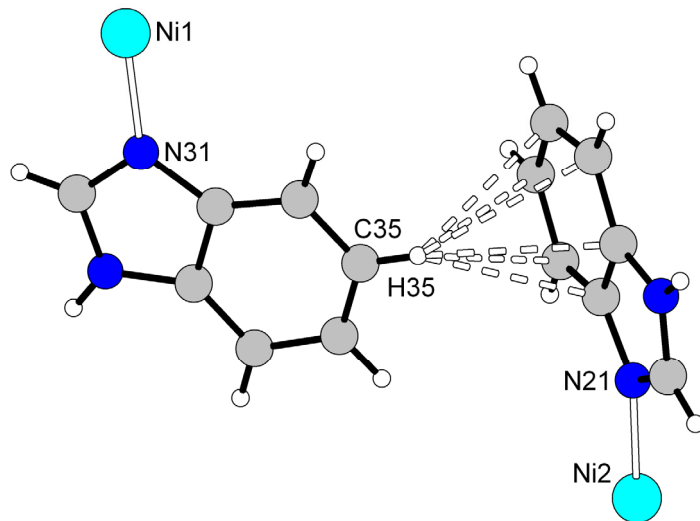


Figure S2 Asymmetric unit and selected symmetry equivalents of **2**. Hydrogen atoms omitted for clarity. Thermal ellipsoids at the 50 % level. Symmetry operators: *i*) $1-x, y, \frac{1}{2}-z$; *ii*) $1\frac{1}{2}-x, 1\frac{1}{2}-y, -z$.

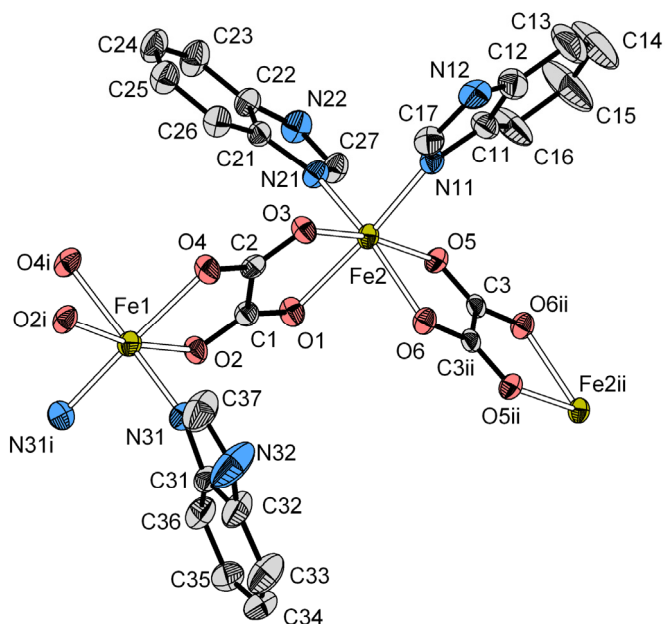


Figure S3 Asymmetric unit and selected symmetry equivalents of **4**. Hydrogen atoms omitted for clarity. Thermal ellipsoids at the 50 % level. Symmetry operators: *i*) $1-x, y, \frac{1}{2}-z$; *ii*) $1\frac{1}{2}-x, 1\frac{1}{2}-y, -z$.

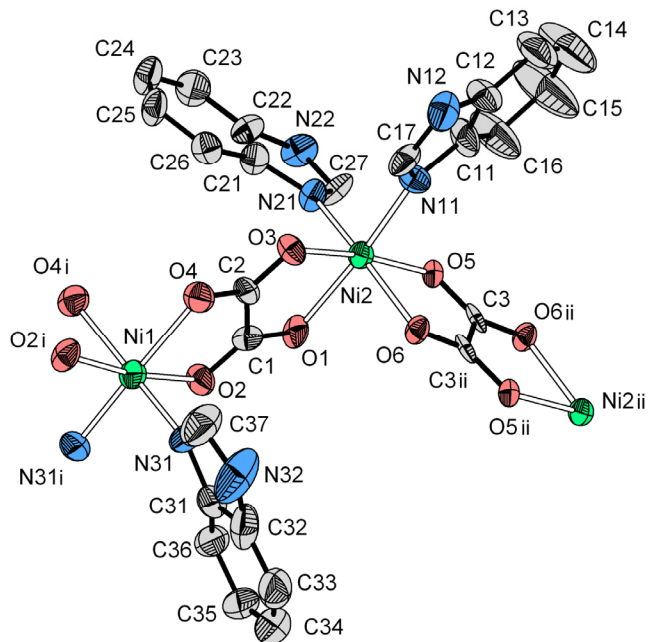


Figure S4 Asymmetric unit and selected symmetry equivalents of **5**. Hydrogen atoms omitted for clarity. Thermal ellipsoids at the 50 % level. Symmetry operators: *i*) $1-x, y, \frac{1}{2}-z$; *ii*) $1\frac{1}{2}-x, 1\frac{1}{2}-y, -z$.

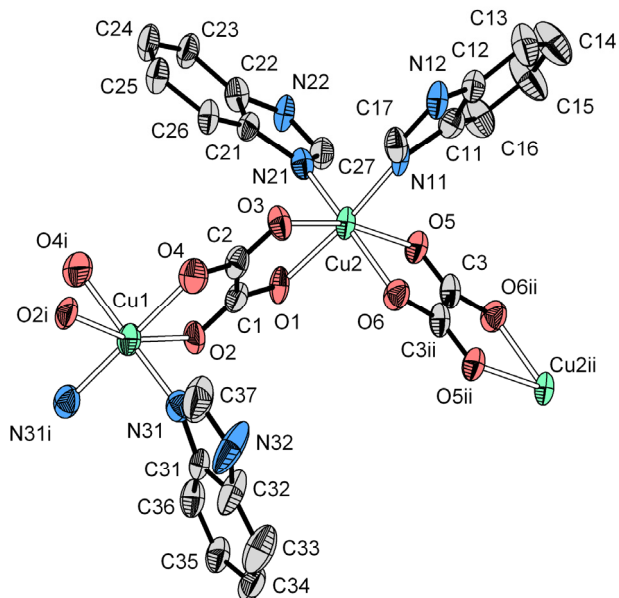


Figure S5 a) Le Bail fit of unit cell to the powder X-ray data of **3**. $C2/c$, $a = 20.673(2)$ Å, $b = 12.546(1)$ Å, $c = 18.127(2)$ Å, $\beta = 93.028(9)^\circ$. b) Le Bail fit of unit cell to the powder X-ray data of **6**. $C2/c$, $a = 21.829(3)$ Å, $b = 12.272(2)$ Å, $c = 18.372(2)$ Å, $\beta = 95.32(1)^\circ$.

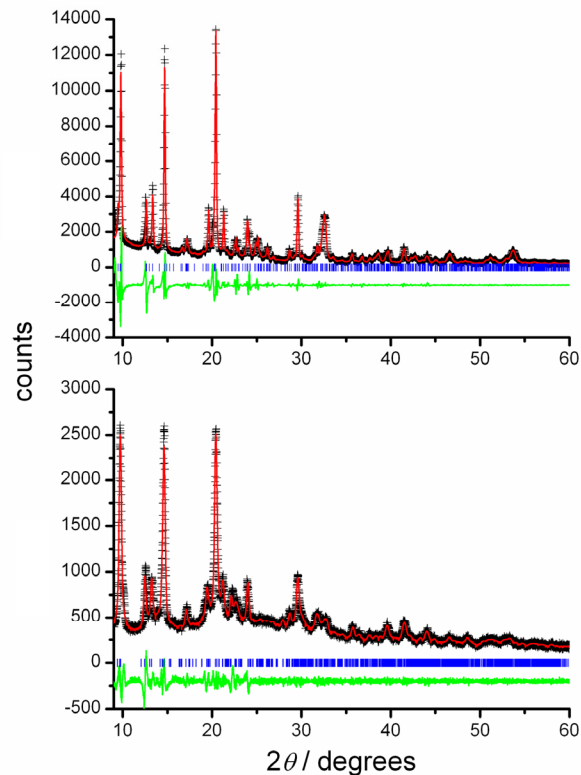


Figure S6 Asymmetric unit and selected symmetry equivalents of **9**. Hydrogen atoms omitted for clarity. Thermal ellipsoids are at the 50 % level. Symmetry operators: i) $x, -y, \frac{1}{2}+z$.

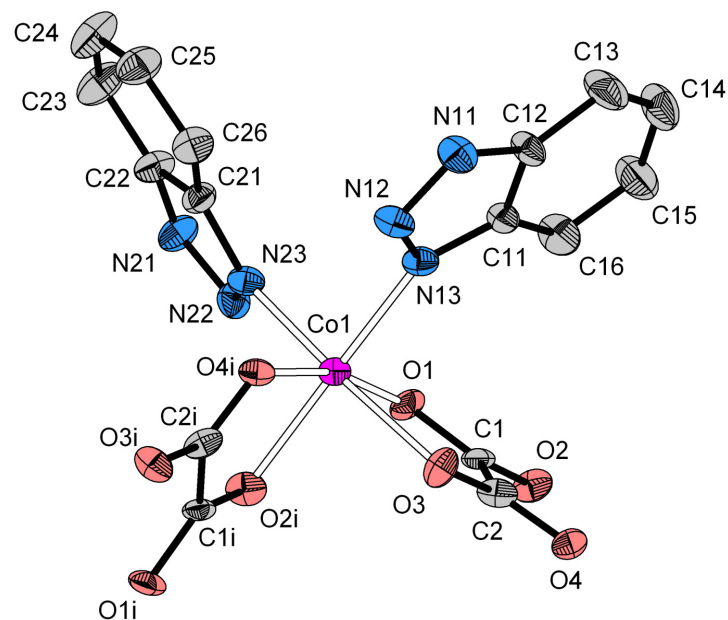


Figure S7 Asymmetric unit and selected symmetry equivalents of **11**. Hydrogen atoms omitted for clarity. Thermal ellipsoids are at the 50 % level. Symmetry operators: $i) x, -y, \frac{1}{2}+z$.

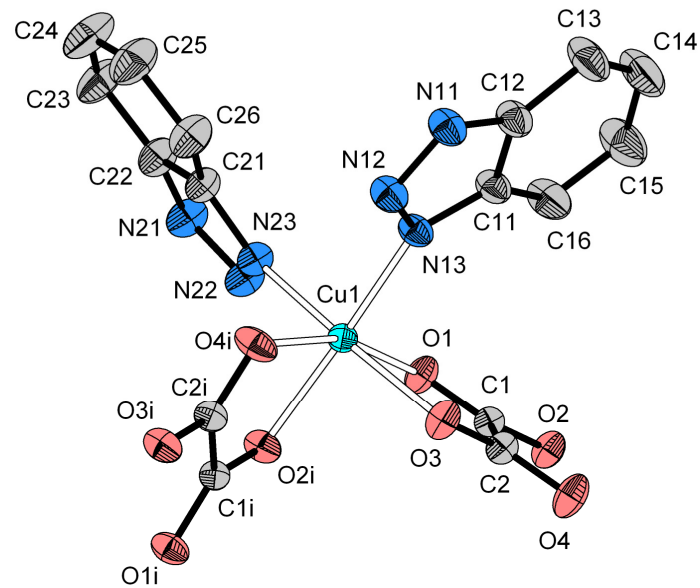


Figure S8 Asymmetric unit and selected symmetry equivalents of **12**. Hydrogen atoms omitted for clarity. Thermal ellipsoids are at the 50 % level. Symmetry operators: $i) x, -y, \frac{1}{2}+z$.

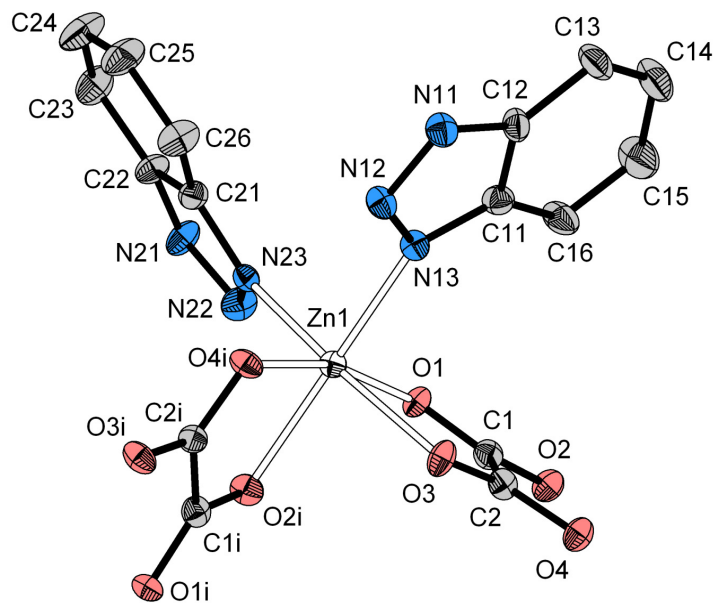


Figure S9 Le Bail fit of unit cell to the powder X-ray data of **10**. Cc , $a = 14.266(2)$ Å, $b = 12.288(2)$ Å, $c = 9.090(2)$ Å, $\beta = 109.176(8)^\circ$.

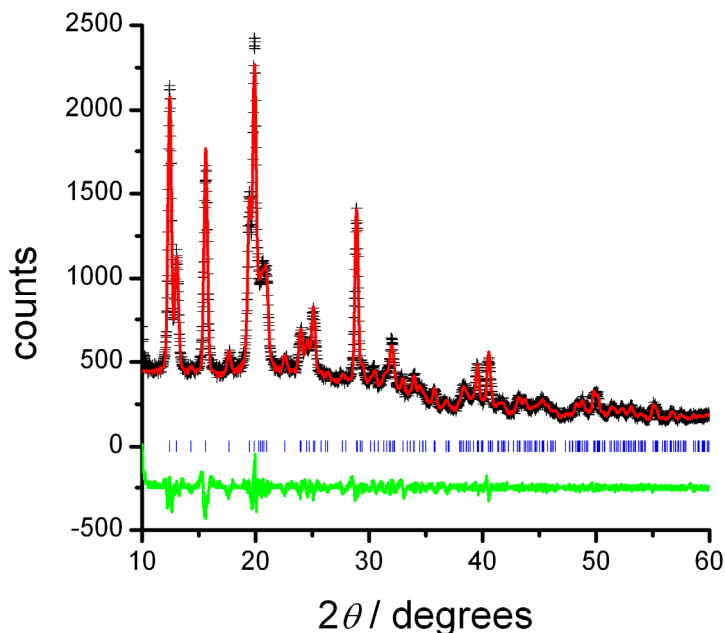


Figure S10 Asymmetric unit and selected symmetry equivalents of **10** as obtained from modelling of the powder X-ray data.

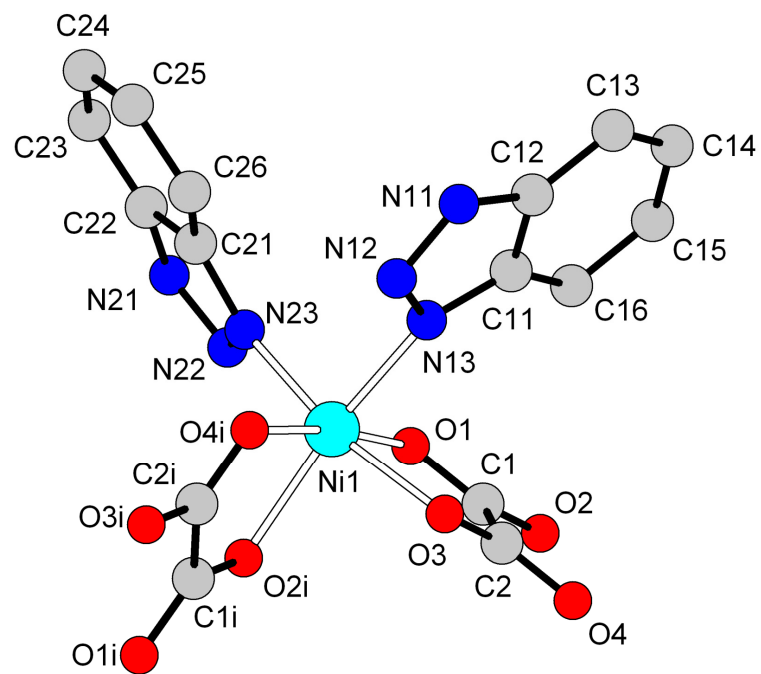


Table S1 Hydrogen bond distances (\AA) and angles ($^\circ$) for **2**

	D–H / \AA	H···O / \AA	D···A / \AA	D–H···O / $^\circ$
N32–H32···O6 <i>i</i>	0.86	2.49	3.18(3)	137.5
N12–H12···O4 <i>ii</i>	0.86	2.18	2.97(3)	153.8
N22–H22···O2 <i>iii</i>	0.86	2.22	3.05(1)	160.5
N22–H22···O1 <i>ii</i>	0.86	2.40	3.06(3)	133.8
C27–H27···O5	0.93	2.35	2.920(6)	119.4
C16–H16···O5	0.93	2.44	3.140(8)	132.4
C26–H26···O3	0.93	2.63	3.39(2)	139.4
C17–H17···O3	0.93	2.57	3.09(1)	116.3
C13–H13···O2 <i>iv</i>	0.93	2.62	3.54(4)	170.3
C23–H23···O1 <i>iii</i>	0.93	2.53	3.214(8)	130.7
C23–H23···O5 <i>iii</i>	0.93	2.60	3.38(2)	141.2

i: 1– x , 2– y , – z ; *ii*: 1– x , 1– y , – z ; *iii*: $1\frac{1}{2}$ – x , $-\frac{1}{2}$ + y , $\frac{1}{2}$ – z ; *iv*: x , 1– y , $-\frac{1}{2}$ + z .

Table S2 Hydrogen bond distances (\AA) and angles ($^\circ$) for **4**

	D–H / \AA	H···O / \AA	D···A / \AA	D–H···O / $^\circ$
N12–H12···O4 <i>ii</i>	0.86	2.43	3.18(1)	146.3
N12–H12···O3 <i>ii</i>	0.86	2.48	3.28(1)	155.0
N22–H22···O2 <i>iii</i>	0.86	2.14	2.97(1)	164.5
N22–H22···O1 <i>ii</i>	0.86	2.51	3.13(1)	130.6
C27–H27···O5	0.93	2.24	2.82(1)	119.5
C16–H16···O5	0.93	2.46	3.14(1)	130.0
C26–H26···O3	0.93	2.59	3.32(1)	135.9
C17–H17···O3	0.93	2.45	2.96(1)	114.5
C13–H13···O2 <i>iv</i>	0.93	2.66	3.58(2)	166.3
C23–H23···O1 <i>iii</i>	0.93	2.45	3.17(1)	133.4
C23–H23···O5 <i>iii</i>	0.93	2.63	3.42(1)	142.7

i: 1– x , 2– y , – z ; *ii*: 1– x , 1– y , – z ; *iii*: $1\frac{1}{2}$ – x , $-\frac{1}{2}$ + y , $\frac{1}{2}$ – z ; *iv*: x , 1– y , $-\frac{1}{2}$ + z .

Table S3 Hydrogen bond distances (\AA) and angles ($^\circ$) for **5**

	D–H / \AA	H···O / \AA	D···A / \AA	D–H···O / $^\circ$
N12–H12···O4 <i>ii</i>	0.86	2.68	3.38(3)	139.0
N12–H12···O3 <i>ii</i>	0.86	2.13	2.96(2)	161.4
N22–H22···O2 <i>iii</i>	0.86	1.98	2.82(2)	166.4
N22–H22···O1 <i>ii</i>	0.86	2.65	3.28(3)	131.6
C27–H27···O5	0.93	2.30	2.92(2)	123.7
C16–H16···O5	0.93	2.49	3.19(2)	132.3
C26–H26···O3	0.93	2.59	3.38(3)	143.6
C17–H17···O3	0.93	2.34	2.98(2)	125.7
C23–H23···O1 <i>iii</i>	0.93	2.50	3.25(2)	138.0
C23–H23···O5 <i>iii</i>	0.93	2.64	3.40(2)	136.6

i: 1– x , 2– y , – z ; *ii*: 1– x , 1– y , – z ; *iii*: $1\frac{1}{2}$ – x , $-\frac{1}{2}$ + y , $\frac{1}{2}$ – z ; *iv*: x , 1– y , $-\frac{1}{2}$ + z .

Table S4 Hydrogen bond distances (\AA) and angles ($^\circ$) for **9**

	D–H / Å	H···A / Å	D···A / Å	D–H···A / °
N11–H11···O1 <i>ii</i>	0.88	1.99	2.87(5)	173.8
C13–H13···O2 <i>ii</i>	0.95	2.37	3.16(5)	150.6
C16–H16···O1	0.95	2.61	3.36(2)	135.2
N21–H21···O4 <i>iv</i>	0.88	1.96	2.84(5)	172.4
C23–H23···O3 <i>iv</i>	0.95	2.63	3.36(4)	134.4

ii: $\frac{1}{2}+x, \frac{1}{2}-y, \frac{1}{2}+z$; *iv*: $-\frac{1}{2}+x, \frac{1}{2}+y, z$.

Table S5 Hydrogen bond distances (Å) and angles (°) for **11**

	D–H / Å	H···A / Å	D···A / Å	D–H···A / °
N11–H11···O1 <i>ii</i>	0.860	1.909	2.769(3)	177.06
C13–H13···O2 <i>ii</i>	0.931	2.481	3.276(3)	143.40
C16–H16···O1	0.930	2.574	3.337(3)	139.69
N21–H21···O4 <i>iv</i>	0.859	1.907	2.764(3)	174.76
C23–H23···O3 <i>iv</i>	0.930	2.613	3.371(3)	139.07

ii: $\frac{1}{2}+x, \frac{1}{2}-y, \frac{1}{2}+z$; *iv*: $-\frac{1}{2}+x, \frac{1}{2}+y, z$.

Table S6 Hydrogen bond distances (Å) and angles (°) for **12**

	D–H / Å	H···A / Å	D···A / Å	D–H···A / °
N11–H11···O1 <i>ii</i>	0.880	1.978	2.853(18)	172.5
C13–H13···O2 <i>ii</i>	0.950	2.399	3.178(13)	139.0
C16–H16···O1	0.950	2.603	3.354(9)	136.2
N21–H21···O4 <i>iv</i>	0.880	1.947	2.823(13)	173.8
C23–H23···O3 <i>iv</i>	0.950	2.599	3.329(12)	133.9

ii: $\frac{1}{2}+x, \frac{1}{2}-y, \frac{1}{2}+z$; *iv*: $-\frac{1}{2}+x, \frac{1}{2}+y, z$.

Table S7 Bond valence sum calculations

Compound	Atom	2+	3+	4+	Result
1	Mn1	2.214	1.959	1.922	2+
	Mn2	2.079	1.917	1.881	2+
7	Mn1	2.125	1.960	1.923	2+
	Fe1	2.047	2.244	—	2+
2	Fe2	2.035	2.235	—	2+
	Fe1	2.094	2.296	—	2+
9	Co1	1.814	1.846	—	2+

† M–L distances taken from reference 4.

Figure S11 Plot of average *cis*-angle against metal type showing increasing tendency towards a regular octahedron from d^5 to d^8 , before increasing again for d^9 and d^{10} .

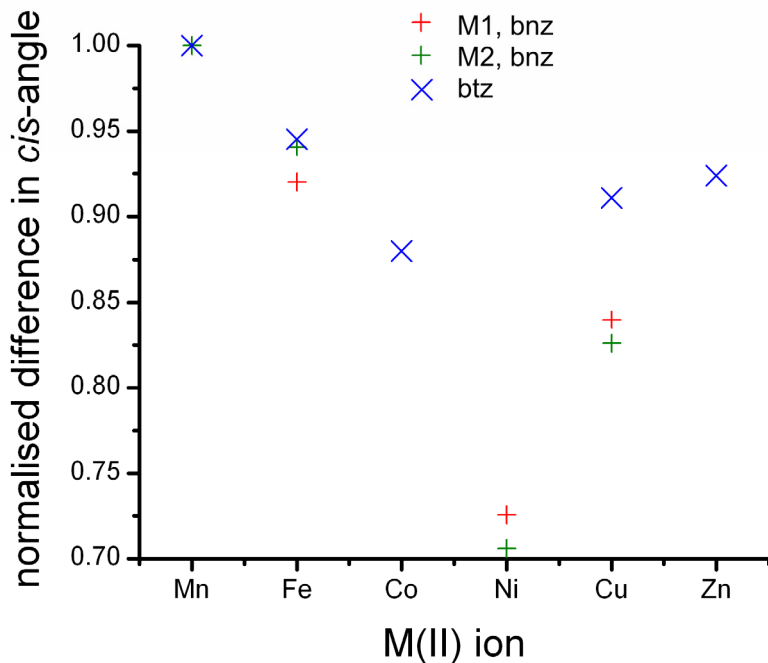


Figure S12 Plot of $\chi(T)$ and $\chi T(T)$ for **7** with fits from the $S = \frac{5}{2}$ Fisher model (equation 2) giving $g = 2.019(4)$ and $J/k_B = -2.86(1)$ K.

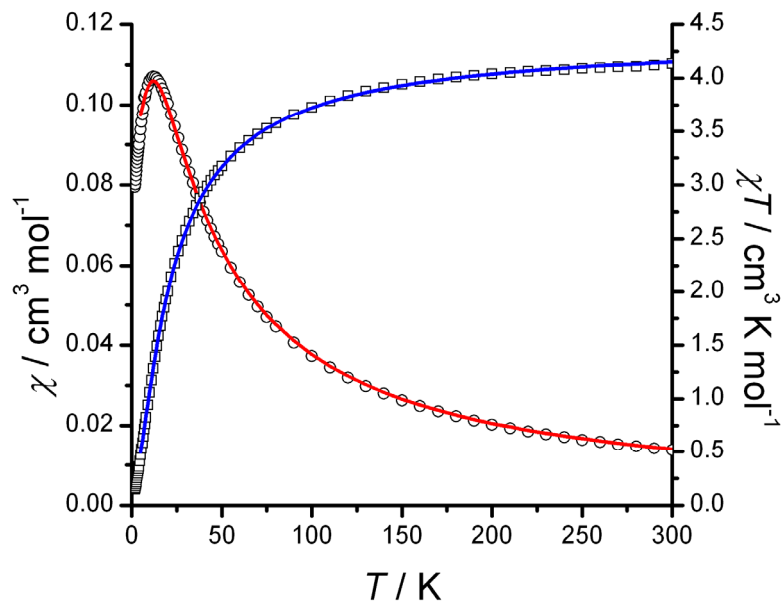


Figure S13 Plot of $\chi(T)$ for **8** with inset showing moment appearing under 15 K.

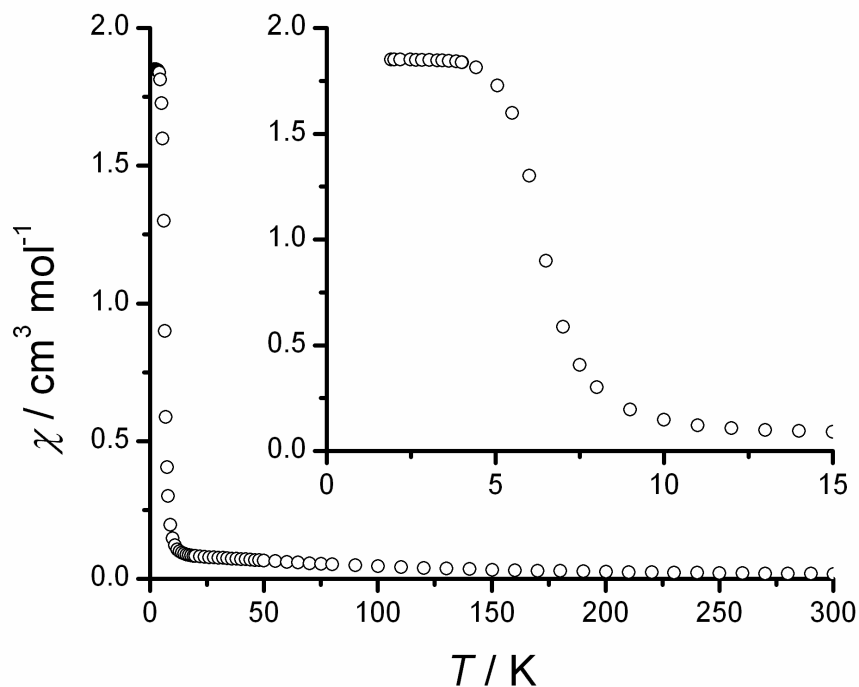


Figure S14 Magnetisation plot for **8** measured at 1.9 K.

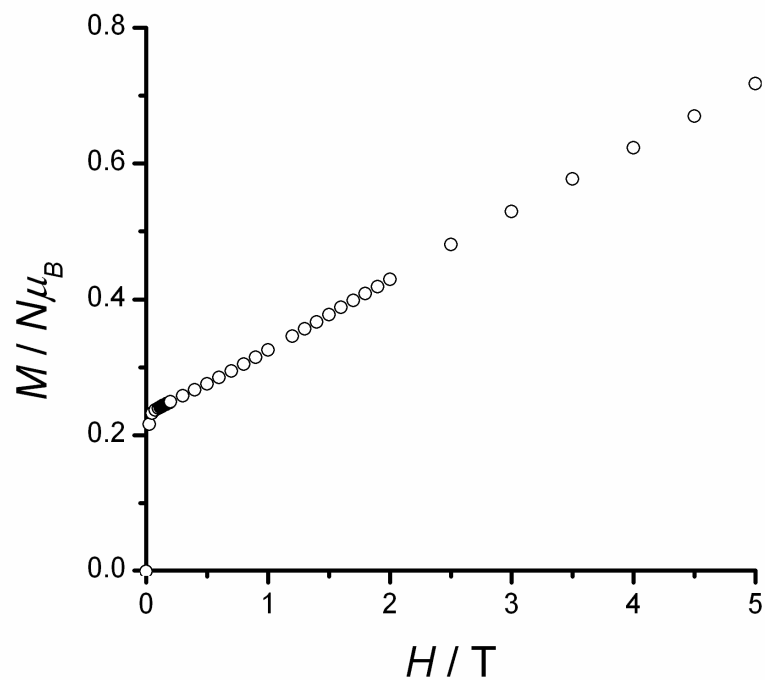


Figure S15 Hysteresis plot for **8** measured at 1.9 K (the line is an eye-guide only).

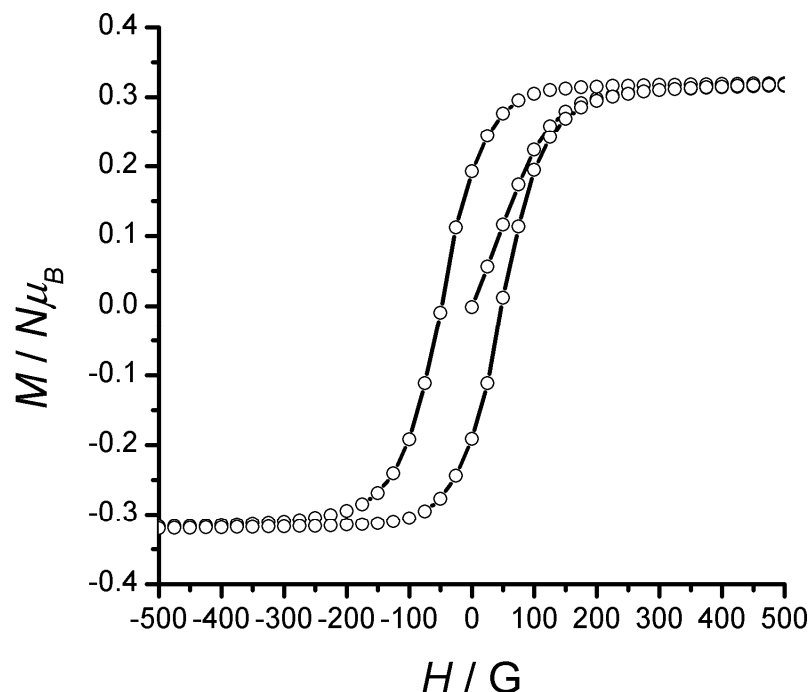


Figure S16 $\chi T(T)$ plot of **8** with fit from the $S = 2$ Ising chain model (equation 3) giving $g = 2.78(1)$ and $J/k_B = -6.7(1)$ K.

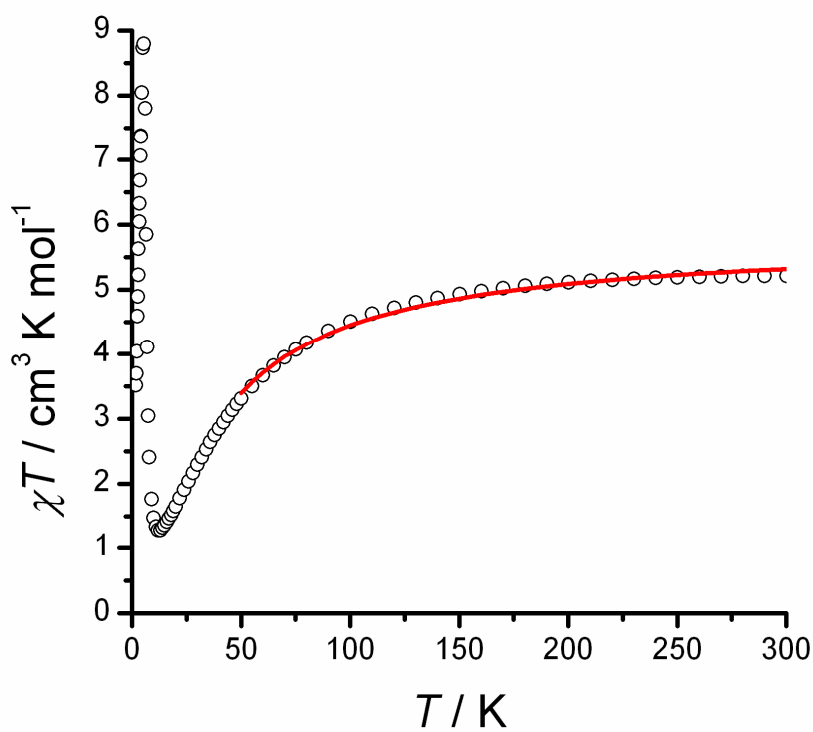


Figure S17 Zero-field cooled (\circ), field cooled (Δ) and remnant (+) magnetisation plots for **8**.

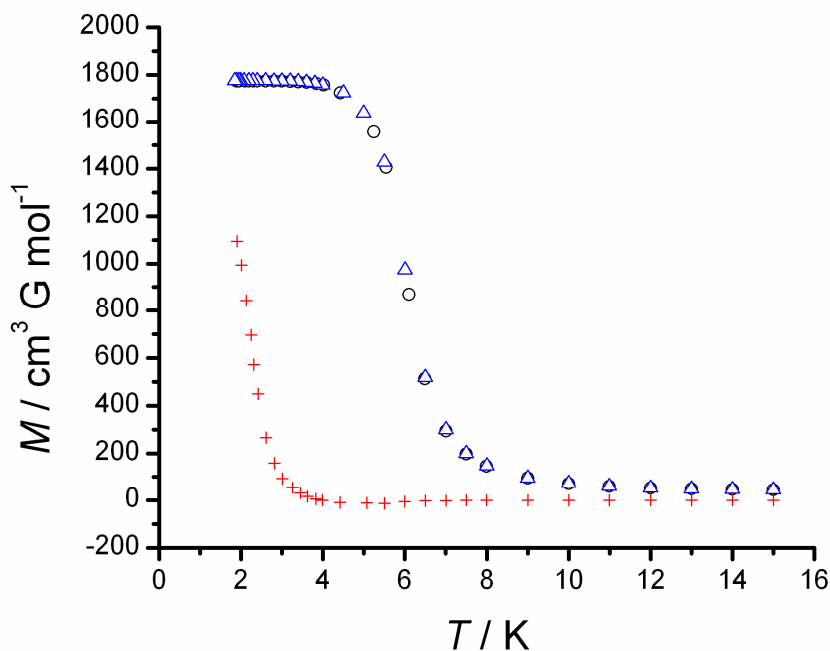


Figure S18 In phase component, $\chi'(T)$, of the AC susceptibility plot of **8**.

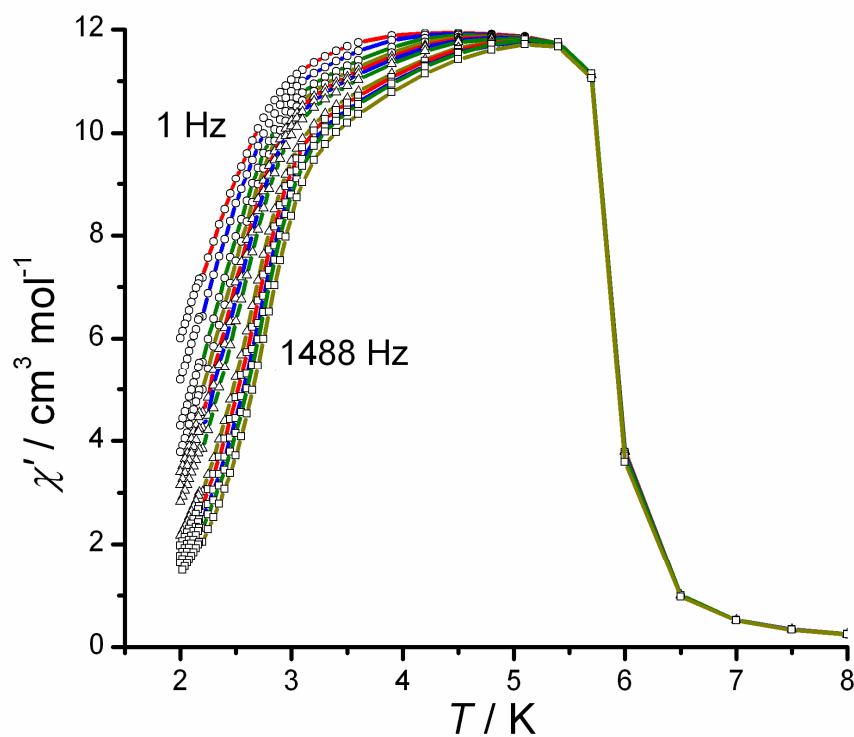


Figure S19 Arrhenius plot (equation 4) for **8** with $E_a/k_B = 62(1)$ K and $\tau_0 = 2(1) \times 10^{-14}$ s.

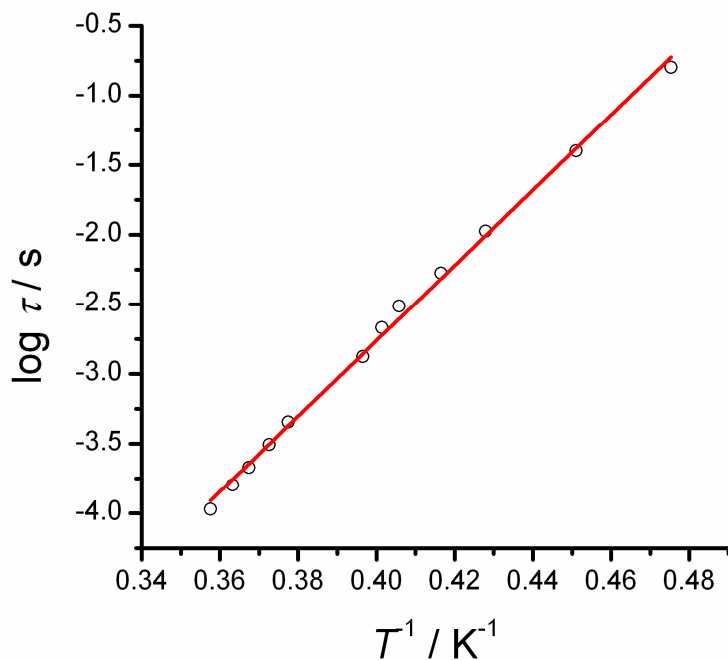


Figure S20 Plot of $\chi(T)$ and $\chi T(T)$ for **9** with fits from the modified Rueff model (equation 6) giving $g = 2.54(1)$, $D/k_B = 87(2)$ K, $\alpha = 1.78(2)$ and $J/k_B = -19.3(2)$ K.

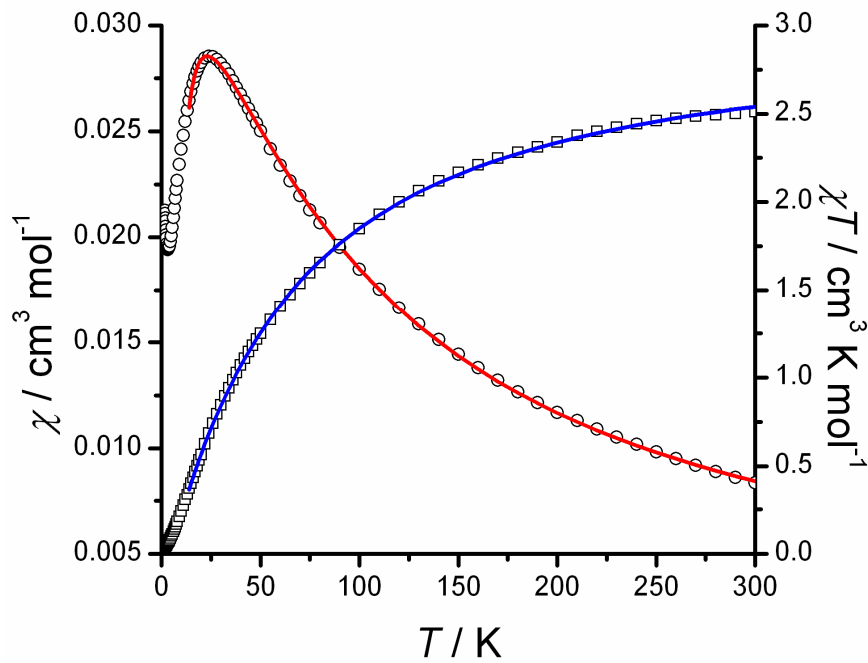


Figure S21 Plot of $\chi(T)$ and $\chi T(T)$ for **10** with fits from the Souletie model (equation 7) giving $g = 2.11(1)$, $J/k_B = -41.1(5)$ K and $p = 4.9(2)$ %.

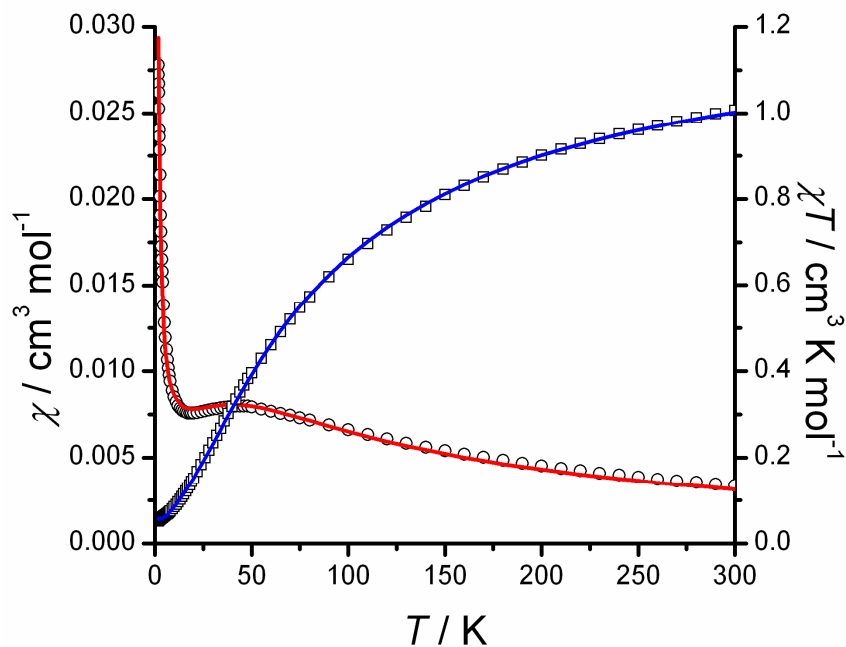


Figure S22 Magnetisation plot for **5** with calculated curve (red line) using the model in figure 15 (main text) in an $n = 12$ ring with $J_1/k_B = +2.50$ K, $J_2/k_B = -2.75$ K and $g = 2.14$. For comparison, a Brillouin curve for an $S = \frac{1}{2}$ uncoupled paramagnet with $g = 2.14$ is included (blue line).

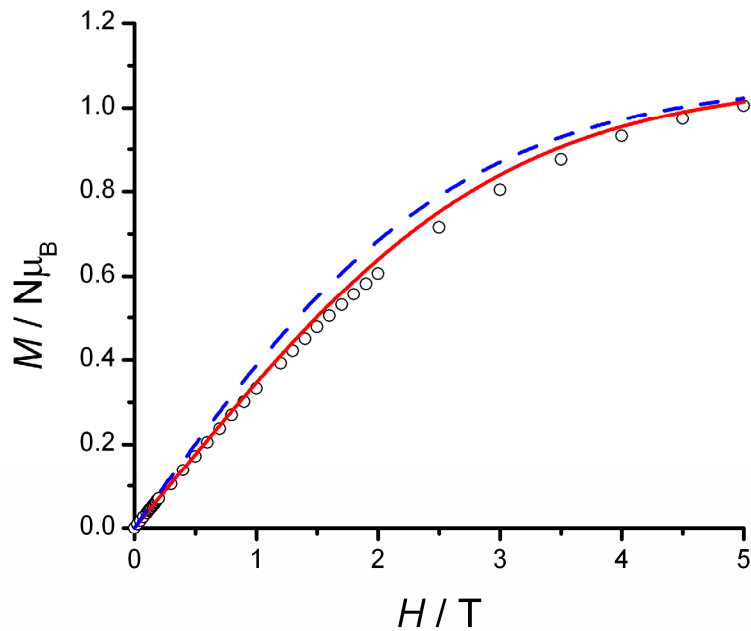
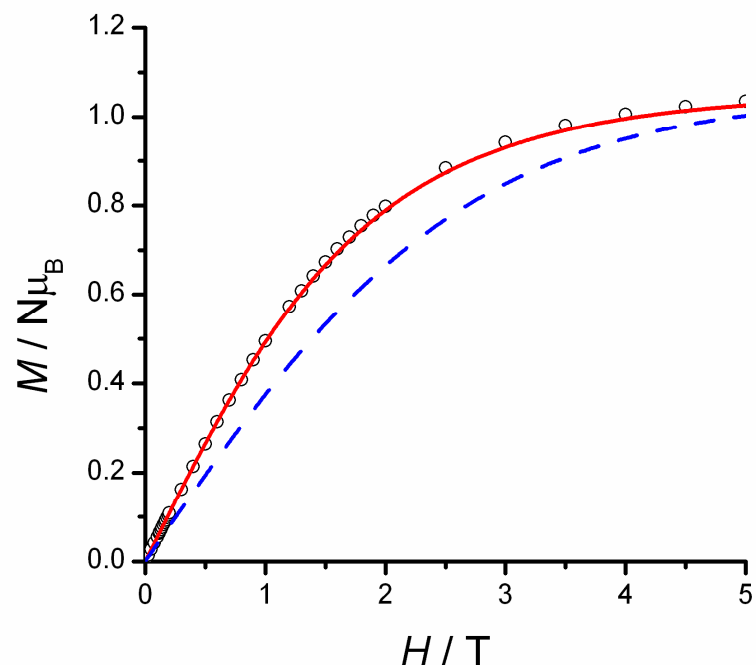


Figure S23 Magnetisation plot for **11** with calculated curve (red line) for an $n = 16$ ferromagnetically-coupled ring with $g = 2.113$ and $J/k_B = +1.49$ K. For comparison, a Brillouin curve for an $S = \frac{1}{2}$ uncoupled paramagnet with $g = 2.113$ is included (blue line).



Synthesis of [Cu(ox)(benz)₂(H₂O)_½(MeOH)_½], 14

Cu(II) acetate monohydrate (1 mmol, 200 mg) and oxalic acid dihydrate (1 mmol, 126 mg) were dissolved in a saturated solution of benzimidazole in methanol and the solution left to stand with a silica TLC plate submerged in it. After 24 hours, blue crystals of the product had formed, which were washed with methanol and acetone before being bottled quickly, due to the loss of methanol on standing.

C_{16.50}H₁₅CuN₄O₅ (412.87 g mol⁻¹): expected: C 48.0; H 3.66; N 13.57. Found C 48.07; H 3.65; N 13.25.

IR (KBr disc, transmission, cm⁻¹): 3431 (s), 3148 (m), 3114 (m), 2985 (w), 2957 (w), 2918 (w), 2845 (w), 1660 (s), 1619 (s), 1603 (s), 1587 (s), 1497 (m), 1421 (w), 1356 (w), 1306 (m), 1274 (m), 1252 (m), 1153 (w), 1110 (w), 1006 (w), 974 (w), 796 (m), 745 (m), 619 (w), 545 (w), 492 (w), 423 (w).

Structure

The structure of **14** consists of one copper atom, one oxalate anion, two benzimidazole molecules and a disordered solvent molecule, which is approximately half water and half methanol. The oxalate anion chelates the copper atom with Cu–O distances of 1.963(19) and 1.958(4) Å, the bond distances indicating that the coordination is taking place in the $d_{x^2-y^2}$ orbital. The remaining two sites of this orbital are occupied by coordination from the two benzimidazole molecules. One lobe of the d_{z^2} orbital is occupied by methanol and water, disordered in an approximately 50:50 ratio. This complex then hydrogen bonds to neighbouring complexes to build the three-dimensional structure.

Table S4 Single-crystal crystallographic parameters for **14**.

Formula	C _{16.50} H ₁₅ CuN ₄ O ₅
Crystal system	Monoclinic
Space group	C2/c
a/Å	20.046(4)
b/Å	10.587(2)
c/Å	17.484(4)
α/Å	90
β/Å	106.30(3)
γ/Å	90
V/Å ³	3561.5(12)
ρ/g cm ⁻³	1.540
T/K	150(2)
μ/mm ⁻¹	1.262
Reflections collected	13619
Unique reflections (R_{int})	3187 (0.0910)
Reflections $F^2 > 2\sigma(F^2)$	2075
Data/Restraints/Parameters	3187/1/239
Goodness of fit (S)	0.920
$R1/wR2$ [$F^2 > 2\sigma(F^2)$]	0.0443/0.1000
$R1/wR2$ (all data)	0.0774/0.1105

Table S5 Hydrogen bond distances (\AA) and angles ($^\circ$) for **14**

	D–H / \AA	H···O / \AA	D···A / \AA	D–H···O / $^\circ$
N4–H4···O1 <i>i</i>	0.860	1.908	2.708(4)	154.17
N2–H2···O3 <i>ii</i>	0.860	1.855	2.698(5)	166.56
O31···O1 <i>iii</i>	—	—	2.745(27)	—
O11···O1 <i>iii</i>	—	—	2.737(25)	—

i: $\frac{1}{2}x, -\frac{1}{2}y, \frac{1}{2}z$; *ii*: $\frac{1}{2}x, \frac{1}{2}y, -z$; *iii*: $\frac{1}{2}x, 1\frac{1}{2}y, -z$.

Figure S24 Asymmetric unit and selected symmetry equivalents of **14**. Hydrogen atoms omitted for clarity. Thermal ellipsoids are at the 50 % level.

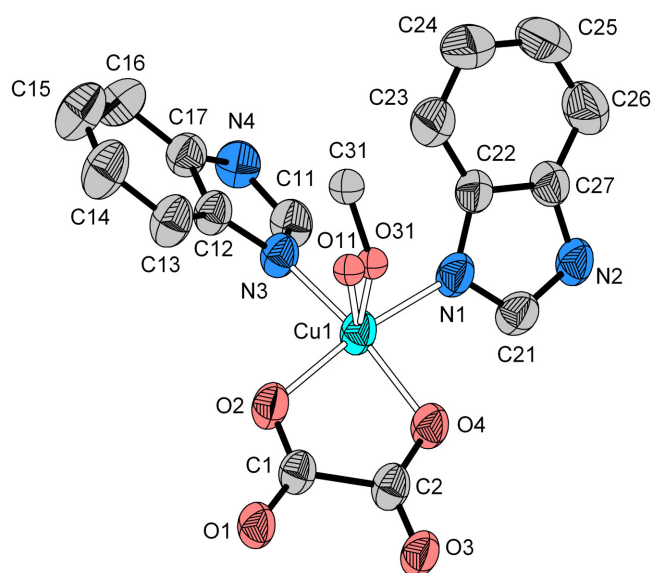


Figure S25 Hydrogen bonding in **14**.

